MBNA Publishing House Constanta 2022

Proceedings of the International Scientific Conference SEA-CONF

SEA-CONF PAPER • OPEN ACCESS

Experimental and numerical investigation regarding the impact behaviour of 7,62 mm bullet steel core with a multilayered armour plate

To cite this article: A. Malciu, C.-C. Puică, G.-F. Noja, B. Krupenschi, Proceedings of the International Scientific Conference SEA-CONF 2022, pg. 26-38.

Available online at www.anmb.ro

ISSN: 2457-144X; ISSN-L: 2457-144X

doi: 10.21279/2457-144X-22-004

Experimental and numerical investigation regarding the impact behaviour of 7,62 mm bullet steel core with a multilayered armour plate

Adrian MALCIU[a, b *], Constantin-Cristinel PUICĂ[a], Gabriel-Flavius NOJA[a], Bogdan KRUPENSCHI[a]

[a] Military Equipment and Technologies Research Agency (METRA).
[b] Doctoral School of Industrial Engineering and Robotics, University Politehnica, Bucharest, Romania.

*Corresponding author: Adrian MALCIU, amalciu@acttm.ro, Center for Research and Innovation for Armament, Military Equipment and Technologies Research Agency, Bucharest, Romania.

Abstract. The development of new and performant armours takes place simultaneously with the production of ammunition with higher characteristics regarding to the depth of penetration and the level of damage caused against the armoured vehicles. Therefore, the current work proposes an experimental and numerical analysis for two impacts between 7,62x54 mm API bullets and a multi-layered armour plate, consisting of ceramic tiles, aramid woven fabric, ultra-high molecular weight polyethylene (UHMWPE) material and a steel plate. Firstly, the armour plate is described presenting the materials of the component layers. Next, the results for the two impacts are emphasized, specifying the impact velocities for each shot and showing the damage resulted in the ceramic layer after impact. In the experimental tests, an apparently disruption of the two bullets was observed at the moment of impact with the ceramic layer. So, the aim of this paper is to investigate the impact behaviour of the bullet core by using the numerical simulation means provided by LS-DYNA finite element program, in order to understand the influence of the high-hardness ceramic layer against the bullet steel core. All the material models used in the numerical simulations were defined accordingly with those found in the literature.

1. Introduction

Nowadays, the military vehicles need to be equipped with more complex protection systems, regarding the evolution of technology in the ammunition field. Even if the actual active systems provide a wide range protection against almost all types of ammunition, a sufficient safety against kinetic energy threats can be obtained only by using passive armour. Taking into consideration the dimensions of these threats and costs effectiveness aspects, it is a difficult way to defeat them by active countermeasures.

The passive armours come with some cost advantages, but the most significant characteristics remains the total mass added to the basic vehicle armour. In the past, the passive protection was based on rolled homogeneous armour (RHA) steel, but with time, the armour piercing bullets were become more efficient against them, having higher values of depth penetration. To defeat this type of ammunitions, a thicker RHA steel armour is needed and higher values of areal density will be obtained. Increasing the total mass of the vehicle, the optimum mobility parameters could be affected. Because of this, the armour developers were researching for new solutions with lower areal density. In order to obtained that goal, materials with lower mass values, but with higher strength and hardening parameters, replaced the single layered homogenous armours, being integrated in multi-layered armour configurations.

The basic principles of multi-layered armour type stay on the effect of penetrator disruption and the absorption of the residual energy of the penetrator after it has been disrupted [1]. In general, high-hardness, brittle materials are used for the impact side. The materials with these parameters, as ultrahigh-hardness steels and ceramics are, disrupt the penetrator bullets or artillery explosive projectiles fragments through plastic deformation, erosion or by shatter effect. [1]

The energy absorbent materials are used as interlayer material or back side material and are described by high ductility and an ability to absorb the energy in flexure [1]. The fibre-reinforced plastics are an example of such type of materials.

For the purpose of developing an optimized configuration of a multi-layered armour, experimental and modelling work needs to be executed. The modelling techniques minimize the number of ballistic tests and can provide an insight into the penetration process [2]. In the literature, there are a lot of scientific papers that present numerical validation of experimental tests by giving the materials model parameters, elements mesh types, failure criteria and also the type of the analysis.

The work done by Serjouei et al. [3, 4] gives an experimental and numerical approach for determination of the ballistic limit velocity (BLV) for a bi-layer ceramic-metal armour at the impact with a cylindrical projectile. Tasdermirci and Tunusoglu [5] made an experimental and numerical research regarding the damage formation in multi-layered armour systems, with and without interlayer, using rubber, Teflon and aluminium foam. The interlayer was arranged between the face ceramic layer and the E-Glass/polyester composite backing plate.

The combination of steel and ceramic, in a steel-encapsulated SiC armour modules, was studied by Goh et al. by conducting an experimental and hydrocode simulation to investigate the correlation between hardness of steel and the ballistic performance of the mentioned armour modules. A conclusion regarding this work was that increasing the hardness of steel cover plate did not improve the ballistic performance [6].

Bhat et al. [7] worked on a review of different armor systems including the multilayered armor ones, in order to understand their response on ballistic impact. An example of such armor presented in their paper consists from a ceramic impact face, an aramid or ramie fiber composite interlayer and an aluminum back layer. This configuration respects the principles outlined upper in this article and referenced in [1].

In this current work, for investigating the projectile and the armor behavior, two bullets impact experiments using a multilayered armor plate made from aluminum alloy plate, 98% purity alumina ceramic tiles, aramid fiber woven, UHMWPE fiber material and a thin high-hardness steel plate, are described. Firstly, the proposed solution of the armor and the experimental setup are presented. The results regarding bullets impact velocity are then utilized for defining the initial condition of the 3D numerical simulation in LS-DYNA. The numerical results are after compared with the experimental ones by taking into consideration the damage of the armor ceramic tiles. This is conducted for validation of the numerical simulation solution. Once the comparison is made, the way how the bullet is disrupted by the high-hardness ceramic tile will be studied for an insight, to understand the disruption or the shatter effect phenomena, that were observed during the experimental tests.

2. Experimental research

2.1. The multilayered armour

The proposed armor plate consists from 5 layers of different materials with a specific role in defeating the incoming kinetic threats. The strike face was made from a 2 mm aluminum alloy plate, then the second layer was build with 50x50x10 mm alumina (Al_2O_3) ceramic tiles arranged in a honeycomb configuration (point *a* from Figure 1). Taking into account that alumina has high hardness value, its role is to disrupt the bullet core.

For the next three layers, 10 mm thick 2D aramid woven fabric (point *b*) and 10 mm thick UHMWPE fiber (point *c*) from Teijin Aramid were used to reduce the spalling effect, retaining the pieces fractured from ceramic tiles and absorbing the kinetic energy of the fragmented core of the bullet, due to its mechanical properties. Another 3 mm thick armor steel plate (point *d*) was used for mounting consideration and as a support for the two composite layers present above. The resulted areal density for this configuration was about 84,16 kg/m^2.

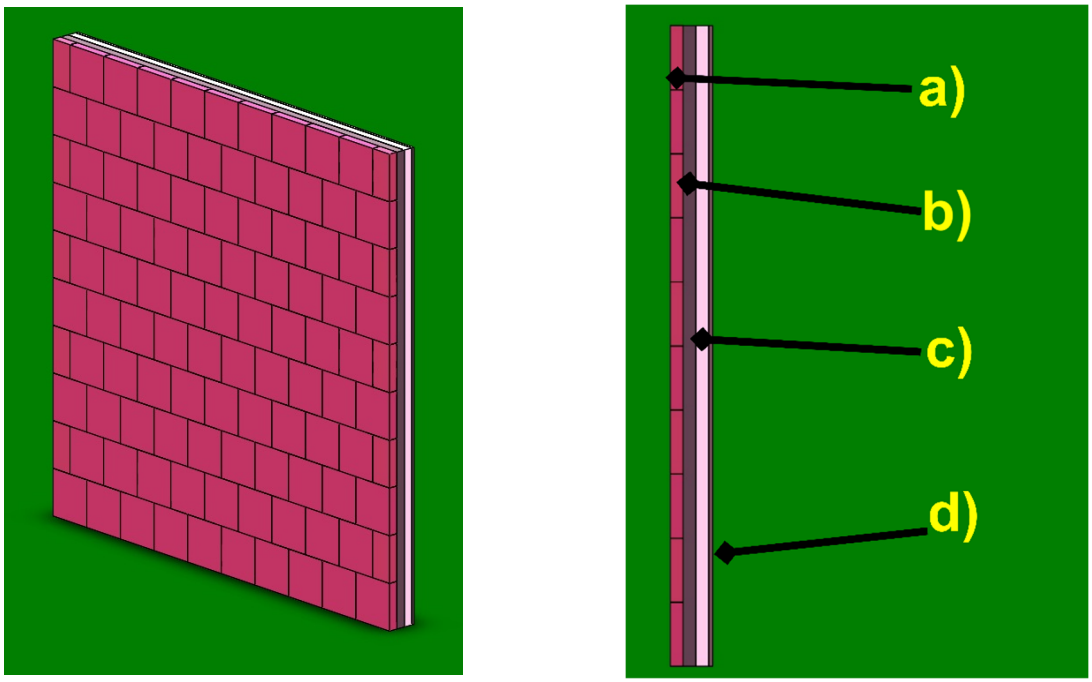

Figure 1. The proposed multilayered armor

The multilayered armor was covered with 1 mm layer of aramid fiber, as will be presented later in this paper. As it can be observed in Figure 1, the aluminum alloy plate has not been represented graphically.

2.2. The experimental setup

The armor plate described in the above section was subjected at 6 impacts with the armor piercing incendiary bullet of 7,62×54 mm cartridge. For all 6 hit points, there was no complete penetration, only the ceramic tiles being broken.

The experimental setup is shown in Figure 2. The 7,62 mm semiautomatic rifle was used for firing the 6 bullets. The armor plate was placed at 30 m from the gun and, between them, a chronograph was arranged at 5 m from the muzzle in order to measure the velocity of each bullet (Figure 3).

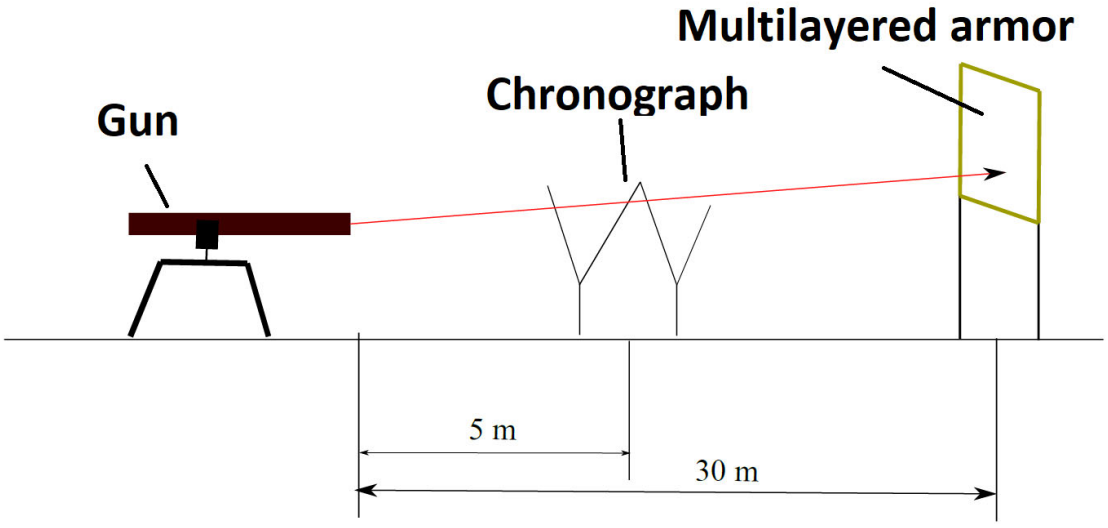

Figure 2. The experimental setup

Figure 3.a. The armor support device

Figure 3.b. The semiautomatic rifle and the chronograph

2.3. 7,62×54 mm API-BZ ammunition

The 7,62×54 mm API-BZ ammunition has a reference bullet in the ballistic protection field. Because of its penetration capacity, it is used for defining the ballistic protection levels in many standards for test procedures of armor materials or armored vehicles.

In Table 1, some of the 7,62×54 API-BZ bullet characteristics are presented.

Table 1. 7,62×54 mm bullet characteristics [15]

	Characteristic	Value / Definition
1.	Muzzle velocity [m/s]	820 (V_{25})
2.	Mass [g]	9,75
3.	Core material	Steel
4.	Jacket material	Bimetal (Tombac)

3. Methodology of numerical simulation

In order to have a global view above the impact phenomena, a three-dimensional FEA model was set. First step for this work was to create the 3D CAD model for the bullet. So, through the means provided by SolidWorks program, the model presented in Figure 4 was build.

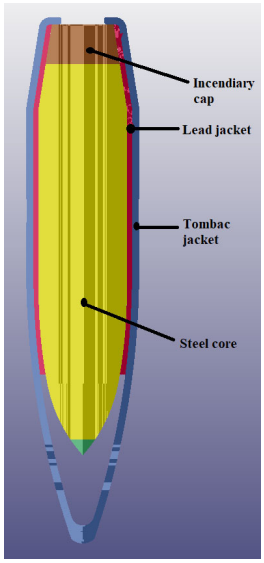

Figure 4. The CAD model of 7,62×54 mm API-BZ bullet, exported in LS-DYNA

Then, the 3D model was imported in ANSYS component, ICEM-CFD, for discretization process. After discretization, a mesh with 1.854.000 hexahedral elements and 1.957.842 nodes was resulted. In Figure 5, the quality and the relative dimensions of the elements are shown.

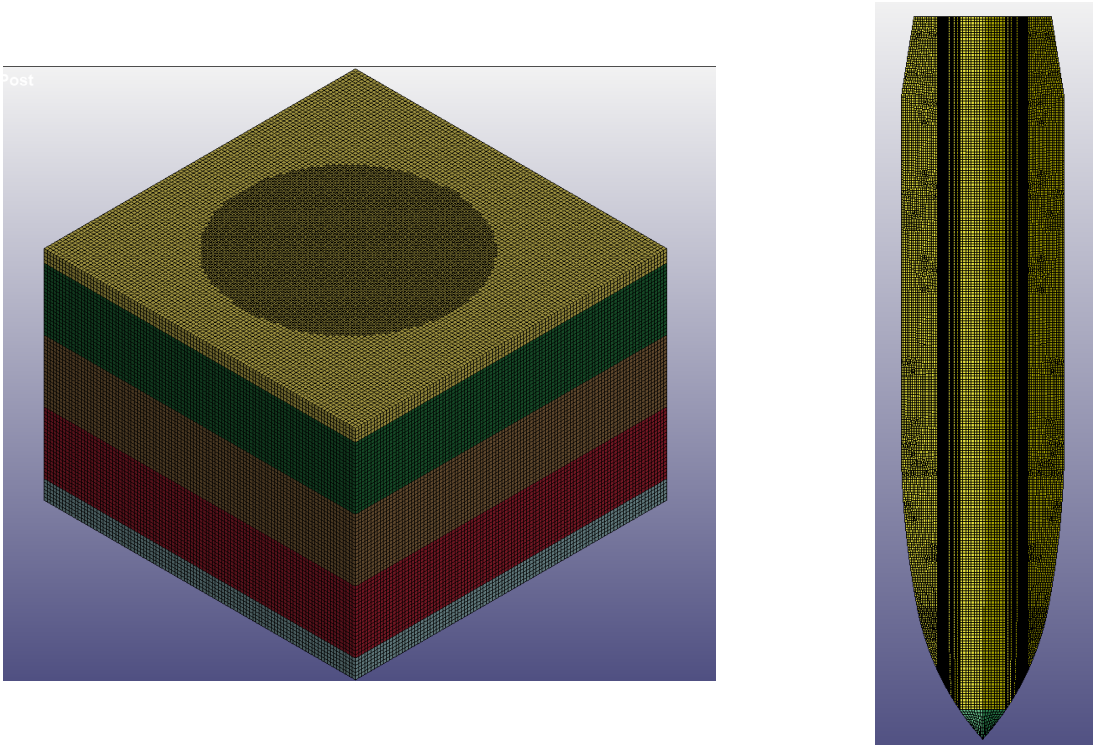

Figure 5. The mesh resulted after discretization

The discretized model was after exported to LS-DYNA PrePost program to define the strength and failure material models for each geometry part. Additionally, the 3D model of the multilayered armor plate was build with the tools provided by LS-DYNA. Also, the discretization was done here, resulting a mesh with 2.432.150 hexahedral elements and 2.579.130 nodes. As can be observed, for minimize the computation time reasons, the model was reduced at the dimensions of one ceramic tile.

Because of the different materials involved in the simulation, different material models were also used to define the strength and the failure criteria for each one. So, for the metallic materials, the Johnson-Cook strength model was applied. For the ceramic tile, the Johnson-Holmquist model was implemented to describe the strength and the failure of alumina. In the case of the two composites, aramid woven and UHMWPE fiber, other two strength and failure model were chosen. For the aramid woven, the Chang-Chang model, defined by *MAT_022 in LS-DYNA, and for UHMWPE, the *MAT_059.

The Johnson-Cook constitutive model was used to reproduce the high strain rates behavior of the metallic components. This model expresses the flow stress as a function of effective plastic strain, strain rate and temperature [8, 9, 10]:

$$\sigma_y = \left(A + B\bar{\varepsilon}^{p^n}\right)(1 + C \ln \dot{\varepsilon}^*)\left(1 - T^{*^m}\right) \quad (1)$$

$$\dot{\varepsilon}^* = \frac{\dot{\bar{\varepsilon}}^P}{\dot{\varepsilon}_0} \quad (2)$$

$$T^* = \frac{T - T_{room}}{T_{melt} - T_{room}} \quad (3)$$

where: A= yield strength; B=strengthening constant; C=strain rate constant; n= strengthening exponent; m=thermal softening factor; $\bar{\varepsilon}^{p^n}$=effective plastic strain; $\dot{\bar{\varepsilon}}^P$=strain rate; ε *=dimensional effective strain

rate; $\dot{\varepsilon}_0$=reference value for the strain rate; T^*=homologated temperature (dimensionless); T_{room}=room temperature; T_{melt}=melting point; T=current temperature.

For the materials involved in this work, two types of Johnson-Cook model implemented is LS-DYNA were used: the *MAT_098 simplified model and *MAT_107, the modified one. As it is shown in [8, 9,10], the modified model takes in to account the Johnson-Cook failure model, that describe the moment of failure by the following relation:

$$\varepsilon_f = \left(D_1 + D_2 e^{D_3 \sigma^*}\right)(1 + D_4 \ln \dot{\varepsilon}^*)(1 + D_5 T^*), \tag{4}$$

$$\sigma^* = \frac{p}{\sigma_{eff}}, \tag{5}$$

where: D_1-D_5=failure parameters; σ^*=stress triaxiality factor; p=pressure, σ_{eff}=effective stress.

The failure occurs when the failure parameter reaches a value of unity:

$$D = \sum \frac{\Delta \bar{\varepsilon}^p}{\varepsilon_f} = 1, \tag{6}$$

where: $\Delta \bar{\varepsilon}^p$=increase in the value of effective plastic strain; ε_f=failure strain.

For the aluminum alloy and armor steel plates, the *MAT_015 Johnson-Cook strength model was applied.

The material parameters defined by Johnson-Cook models are shown in Table 2.

Table 2. The values of Johnson-Cook parameters [9, 11]

Parameter	Steel core	Tombac Jacket	Lead jacket	Incendiary cap	Aluminum plate	Steel plate
ρ [g/cm^3]	7,85	8,96	11,34	2	2,7	7,85
E [GPa]	210	124	16	7	70	207
ν [-]	0.33	0,34	0,42	0,30	0,3	0,33
C_p [J/kgK]	-	385	-	-	910	450
T_m [K]	-	1356	-	-	893	1800
Strength model	*MAT_098	*MAT_107	*MAT_098	*MAT_098	*MAT_015	*MAT_015
A [Gpa]	1,976	0,206	0,024	0,078	0,167	1,58
B [Gpa]	2,856	0,505	0,300	0,160	0,596	0,958
n [-]	0,207	0,310	1	1	0,551	0,175
C [-]	0,005	0,025	0,1	0	0,001	0,0087
m [-]	-	1,09	-	-	0,859	0,712
Failure parameters						
D_1	-	0,540	-	-	0,0261	0,068
D_2	-	4,88	-	-	0,263	5,328
D_3	-	-3,03	-	-	-0,349	-2,554
D_4	-	0,014	-	-	0,247	0
D_5	-	1,12	-	-	16,8	0,35
*MAT_ ADD_EROSION	MNPRES=-2,6 EPSSH=1 VOLEPS=0,05	VOLEPS=0,2 EPSSH=1	VOLEPS=0,5 EPSSH=1	VOLEPS=0,01 EPSSH=1	-	-

For the ceramic tile, the Johnson-Holmquist (J-H) model, *MAT_110, was used to describe the 98 % purity alumina. This model was chosen because it was widely used in many works to define the brittle behavior of ceramic materials type, such as glass or other ceramic-based materials.

Three equations govern the J-H strength model, as follows:

a) for undamaged material:

$$\sigma_i(p, \dot{\varepsilon}) = A_{J-H}\sigma_{HEL}\left(\frac{T-p}{p_{HELL}}\right)^{D_2}\left[1 + C_{J-H}ln\left(\frac{\dot{\varepsilon}}{\dot{\varepsilon_0}}\right)\right], \quad (7)$$

b) for damaged material:

$$\sigma_i(p, \dot{\varepsilon}) = B_{J-H}\sigma_{HEL}\left(\frac{p}{p_{HELL}}\right)^{M_{J-H}}\left[1 + C_{J-H}ln\left(\frac{\dot{\varepsilon}}{\dot{\varepsilon_0}}\right)\right], \quad (8)$$

c) failure model:

$$\varepsilon_p^f(p) = D_1\left(\frac{T-p}{p_{HELL}}\right)^{D_2}, \quad (9)$$

where: p_{HEL} = pressure for the yield point of Hugoniot; σ_{HEL} = stress for the actual yield point of Hugoniot; A_{J-H} = strength constant of the intact material; N_{J-H}= strength exponent of the intact material; C_{J-H} = strain rate constant; B_{J-H} = strength constant of the damaged material; M_{J-H} = strength constant of the damaged material; D_1 and D_2 = the constant and the exponent of failure respectively [9].

The model parameters for alumina are presented in Table 3.

Table 3. Parameters for Johnson-Holmquist model [9]

Parameter	**Alumina [Al_2O_3]**
ρ [g/cm^3]	3,84
G [GPa]	93
A [-]	0,93
B [-]	0,31
C [-]	0,007
m [-]	0,6
n [-]	0,64
EPSI	1
T [GPa]	0,262
SFMAX [GPa]	1
HEL [GPa]	8
PHEL [GPa]	1,46
Beta	1
D_1 [-]	0.01
D_2 [-]	0,7
K_1 [GPa]	131
K_2 [GPa]	0
K_3 [GPa]	0
*MAT_ADD EROSION	VOLEPS=0.05

The Chang-Chang composite failure model, *MAT_022 in LS-DYNA, was used to simulate the material behavior for the aramid woven layer. In Table 4, the material parameters used in the numerical simulation are presented [12].

Table 4. Aramid parameters for *MAT_022 [12]

Parameter	Value
ρ [g/cm^3]	1,23
EA [GPa]	20,44
EB [GPa]	8,90
EC [GPa]	8,90
PRBA	0,31
PRCA	0,31
PRCB	0,49
G_{AB} [GPa]	1,64
G_{BC} [GPa]	3,03
G_{CA} [GPa]	1,64
Shear strength, *SC* [GPa]	0,34
Longitudinal tensile strength, *XT* [GPa]	1,145
Transverse tensile strength, *YT* [GPa]	0,13
Transverse compressive strength, *YC* [GPa]	0,65

For the UHMWPE layer, composite failure solid model, *MAT_059 type, was chosen. Because the data that describe the constitutive model of Endumax do not exist, the parameters for Dyneema HB26 was selected [13]. For this material, the next parameters, outlined in Tabel 5, was introduced in the program.

Table 5. UHMWPE parameters for *MAT_059 [13]

Parameter	Value
ρ [g/cm^3]	0,97
EA [GPa]	34,257
EB [GPa]	34,257
EC [GPa]	3,26
PRBA	0
PRCA	0,013
PRCB	0,013
G_{AB} [GPa]	0,1738
G_{BC} [GPa]	0,5478
G_{CA} [GPa]	0,5478
In plane shear strength, S_{BA} [GPa]	0,0018
Transverse shear strength, S_{CA} [GPa]	0,0018
Transverse shear strength, S_{CB} [GPa]	0,0018
Longitudinal compressive strength, *XXC* [GPa]	1,25
Transverse compressive strength, *YYC* [GPa]	1,25
Normal compressive strength, *ZZC* [GPa]	1,25
Longitudinal tensile strength, *XXT* [GPa]	1,25
Transverse tensile strength, *YYT* [GPa]	1,25
Normal tensile strength, *ZZT* [GPa]	1E+20

Beside the material defining, the correct selection of contacts between components is a very important step. Thus, regarding the expecting deformation of the layers, the *CONTACT_TIED_SURFACE_SURFACE was defined for the interfaces between component layers of the armor. In the case of contact between the bullet and the multilayered armor, the *CONTACT_ERODING_NODES_TO_SURFACE was modelled, being defined for each plate of the armor. The self-contact between parts of the same body, the *CONTACT_ERODING_SINGLE_SURFACE algorithm was used.

Another step for configuration of the numerical simulation was to set the physical boundaries of the armor plate. So, the plate was fixed with the *BOUNDARY_SET_SPC keyword option, selecting only the nodes from side surfaces of each layer. Additionally, in order to permit the transmission of the shock waves resulted after the ballistic impact, the *BOUNDARY_NON_REFLECTING keyword was defined on the segments from sides surfaces of each layer.

Because of lack of information regarding the yaw angle of the bullet, it was assumed that the bullet hits the target perpendicular on its surface, with 0º yaw angle.

4. Results

4.1. Experimental results

Figure 6.a presents the impact points after the 6 rounds firing. As it can be observed in Figure 6.b, no complete penetration was occurred. In this work, because the integrity of the ceramic tiles was affected during the dismounting operations, only the point 1 and point 3, marked on Figure 6.a, were selected for analysis.

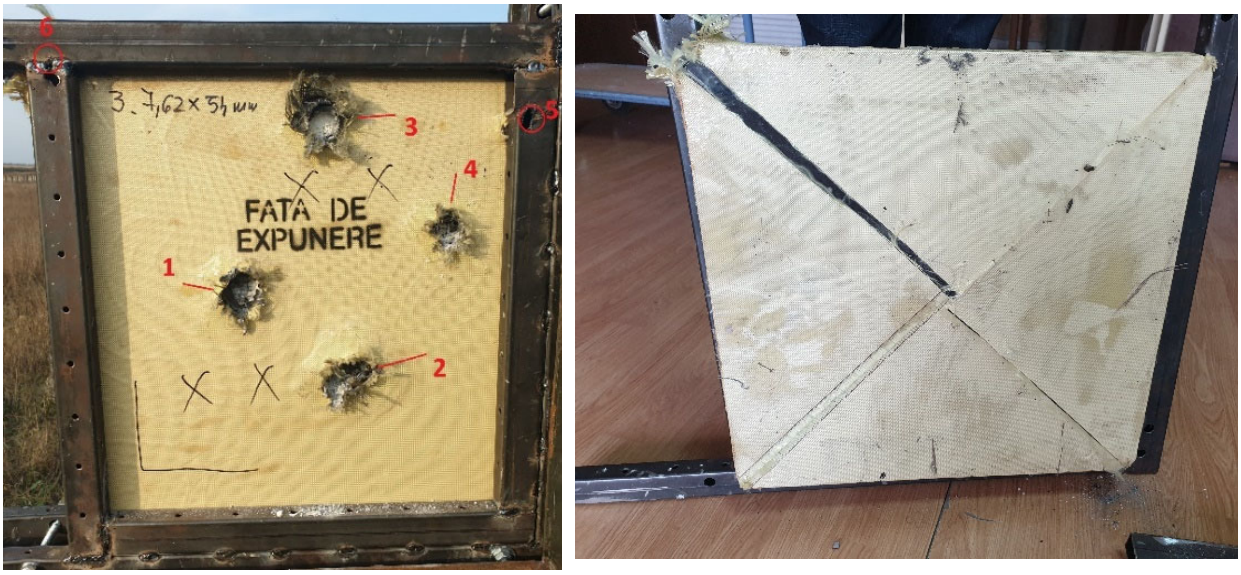

Figure 6. The multilayered armor plate after the 6 bullets firing

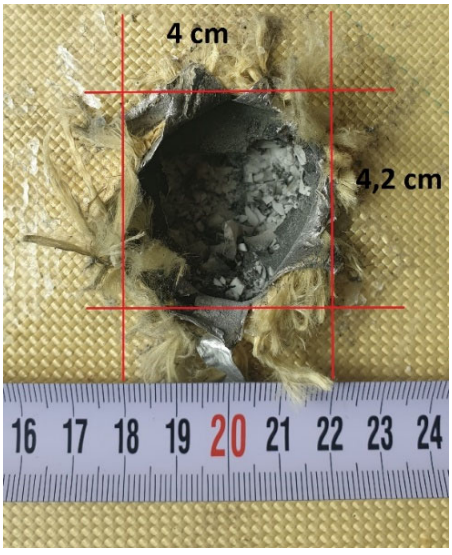

Figure 7. First impact point

In the case of Point 1, the impact evaluated velocity was approximately 804 m/s. In the image from Figure 7, the dimension of the crater formed in the alumina tiles and also the diameter of the hole in the aluminum alloy plate are emphasized

The depth of penetration in the ceramic tile was about 6 mm.

In the case of Point 2, the impact evaluated velocity was approximately 805 m/s. As it was previously presented, in the image from Figure 8, the dimension of the crater formed in the alumina tiles and also the diameter of the hole in the aluminum alloy plate are shown.

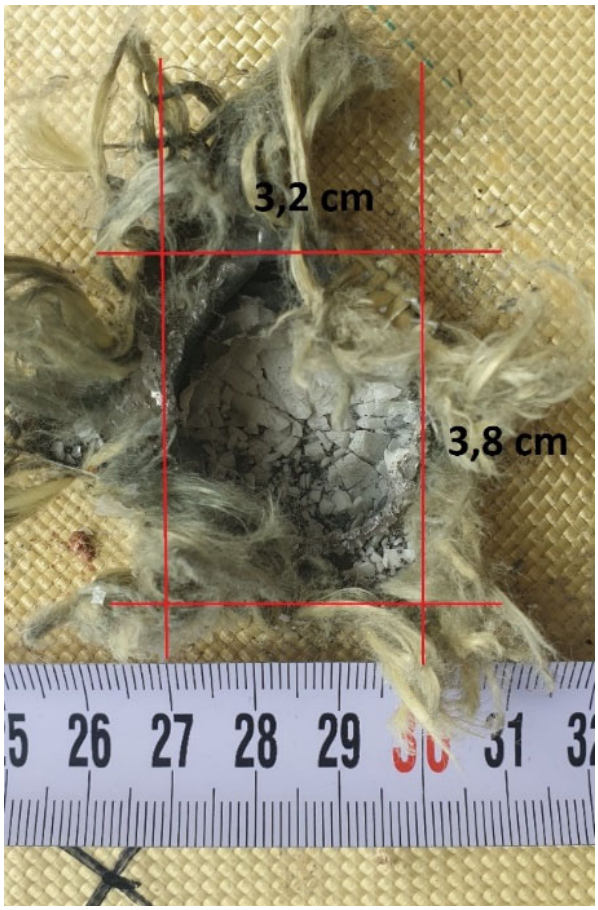

Figure 8. Second impact point

The depth of penetration in the ceramic tile was about 5 mm.

The rest of the ceramic tile was expelled apart from the armor during the unmounting of the armor plate from the support and, also, during the transportation to the laboratory.

4.2. Numerical simulation results

The scope of the numerical simulation was to capture the impact behavior of bullet materials and alumina cracking phenomena in order to understand the way multilayered armor was defeated the two bullets.

As it was previously mentioned, the impact velocities of the bullets were 804 m/s and 805 m/s respectively. For this analysis, the value of 805 m/s was chosen and set by *INITIAL_VELOCITY_GENERATION keyword.

After $t=3,5 \cdot 10^{-2}$ *ms*, the simulation was stopped. In Figure 9, the state of deformation for all bodies is presented. In the case of alumina, the cone outlined in [14] can be observed.

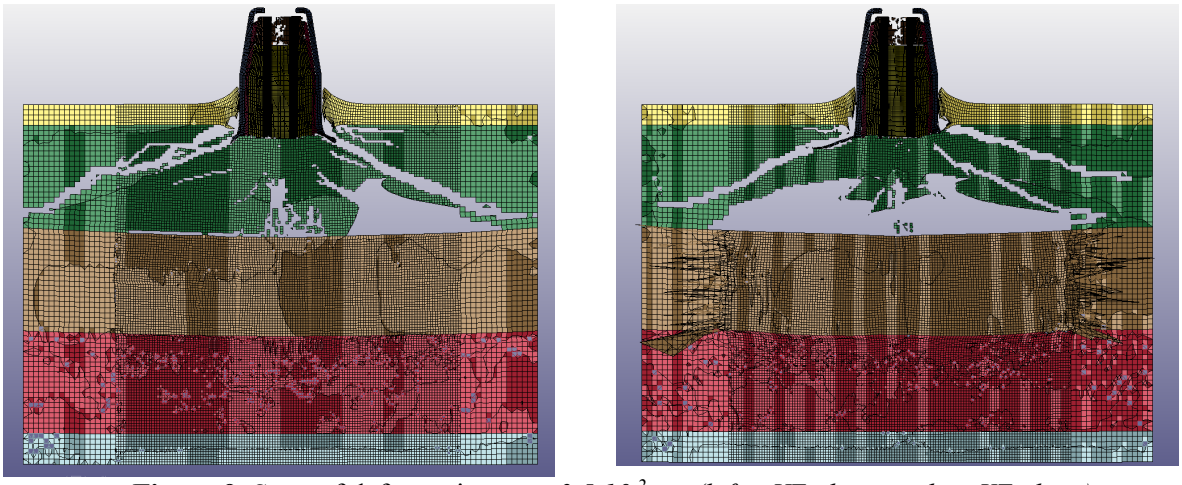

Figure 9. State of deformation at $t=3,5\cdot10^{-2}$ *ms (left – XZ plane, right – YZ plane)*

The damage level of alumina tile is presented in Figure 10.

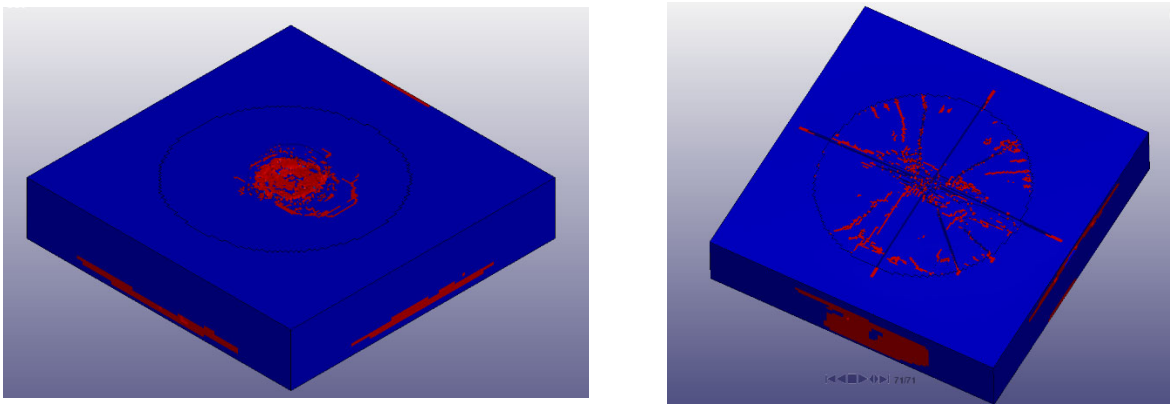

Figure 10. Damage level of alumina tile (left – front face, right – back face)

It can be observed that the failure criteria for the bullet core was reached and also the erosion parameters set by *ADD_EROSION_000 options were activated by reaching the values introduced as in Table 2 and Table 3. The decision to stop the running of the simulation was made for that reason and because the kinetic energy of the bullet core was eroded significantly. With almost more than 70 % eroded mass from the bullet, it can be assumed that there no bigger penetration could take place (see Figure 11).

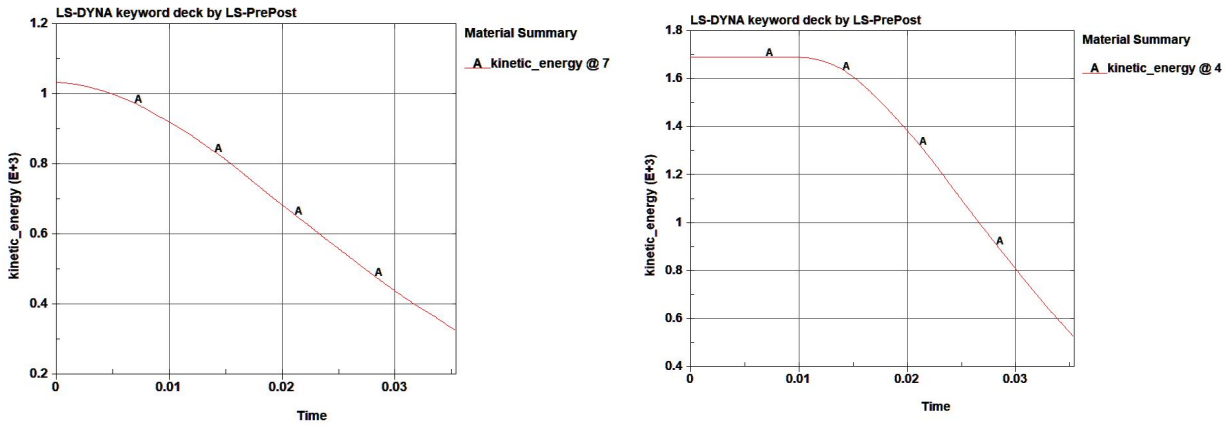

Figure 11. The kinetic energy graph for tombac jacket (left) and steel core (right)

Interesting to investigate is the way how the alumina tiles was broken and to make a comparison with the dimensions of the crater resulted in experimental tests. In the next subsection, an evaluation of the cone formed in the alumina tiles and also the hole depth resulted after impact are analyzed in comparison with the experimental ones.

4.3. Comparison between experiments and numerical simulation

In Figure 12, the broken cone formed from the ceramic tile can be observed from XZ and YZ plane respectively. The red lines were drawn for evaluation reason in order to see the depth dimension. For this scope, the line *OD* designate the height of the cone, that was still remain on the aramid layer. As it can observed, the length of the line OD has a value between 4 to 5 mm.

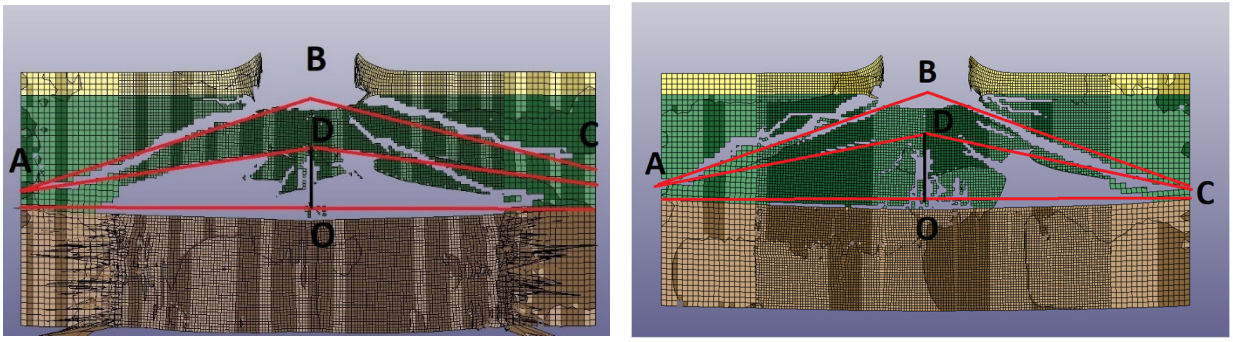

Figure 12. The way ceramic tile was broken by the API bullet in numerical simulation *(left – XZ plane, right – YZ plane)*

As it is said in [9] a satisfactory correlation is can be assigned to an error with values in 10 - 25% interval. In this current work, the difference between experimental results and those from numerical simulation is situated in a relative error of approximately 20 %. So, the simulation presents a satisfactory correlation with the experimental ones.

5. Conclusions

The obtained level of relative error proves the effectiveness of the finite element analysis method in pretesting techniques. The material models used in the numerical simulation and the comparison between the experimental ones gave a satisfactory validation of the model used.

Now, this model can be applied on other applications and can provide a good evaluation regarding the correct configuration of a future armor.

However, the way how the elements of the bullet were eroded still remains a problem to be resolved and this opens future research directions. One of them is to run a series of mechanical tests with the scope of characterization of the bullet materials and, also, the armor materials that form a specific plate. Once every material is described, the parameters obtained from the real tests could be introduced in strength or failure models from FEA program in order to define constitutive model for future ballistic impact.

Acknowledgements

This research was funded by Research and Development Sectorial Plan of the Romanian Ministry of National Defence. Also, the authors gratefully thank to STIMPEX S.A. for the help given in manufacturing the armor plate.

References

[1] CROUCH, Ian (ed.). *The science of armour materials*. Woodhead Publishing, 2016.

[2] DOROGOY, A.; RITTEL, D.; BRILL, A. *Experimentation and modeling of inclined ballistic impact in thick polycarbonate plates.* International Journal of Impact Engineering, 2011, 38.10: 804-814.

[3] SERJOUEI, Ahmad, et al. *Experimental validation of BLV model on bi-layer ceramic-metal armor*. International Journal of Impact Engineering, 2015, 77: 30-41.
[4] SERJOUEI, Ahmad, et al. *On improving ballistic limit of bi-layer ceramic–metal armor.* International journal of impact engineering, 2017, 105: 54-67.
[5] TASDEMIRCI, A.; TUNUSOGLU, G. *Experimental and numerical investigation of the effect of interlayer on the damage formation in a ceramic/composite armor at a low projectile velocity.* Journal of Thermoplastic Composite Materials, 2017, 30.1: 88-106.
[6] GOH, W. L., et al. *Effects of hardness of steel on ceramic armour module against long rod impact.* International Journal of Impact Engineering, 2017, 109: 419-426.
[7] BHAT, Aayush, et al. *Advancement in fiber reinforced polymer, metal alloys and multi-layered armour systems for ballistic applications–A Review.* Journal of Materials Research and Technology, 2021, 15: 1300-1317.
[8] HALLQUIST, John. *LS-DYNA Theory Manual.* Livermore Software Technology Corporation, March 2006.
[9] ZOCHOWSKI, Pawel, et al. *Comparison of Numerical Simulation Techniques of Ballistic Ceramics under Projectile Impact Conditions.* Materials, 2021, 15.1: 18.
[10] JOHNSON, G.R.; COOK, W.H. *Fracture characteristics of three metals subjected to various strains, strain rates, temperatures and pressures*. Eng. Fract. Mech. 1985, 21, 31–48.
[11] KILIÇ, Namık, et al. *Ballistic behavior of high hardness perforated armor plates against 7.62 mm armor piercing projectile.* Materials & Design, 2014, 63: 427-438.
[12] FELI, S.; ASGARI, M. R. *Finite element simulation of ceramic/composite armor under ballistic impact.* Composites Part B: Engineering, 2011, 42.4: 771-780.
[13] HAZZARD, Mark K., et al. *Finite element modelling of Dyneema® composites: from quasi-static rates to ballistic impact.* Composites Part A: Applied Science and Manufacturing, 2018, 115: 31-45.
[14] HAZELL, Paul J. *Armour: materials, theory, and design*. CRC press, 2015.
[15] https://romarm.ro/wp-content/uploads/2021/04/19_Datasheet-Caliber-7.62-x-54-mm.pdf .